Pharmaceutical Research, Vol. 23, No. 3, March 2006 (© 2006)
DOI: 10.1007/s11095-006-9568-2

Research Paper

Voltage Dependence of Transepithelial Guanidine Permeation Across Caco-2 Epithelia Allows Determination of the Paracellular Flux Component

Georgina Carr,[1] Iain S. Haslam,[1] and Nicholas L. Simmons[1,2]

Received June 15, 2005; accepted November 21, 2005

Purpose. The aim of this study was to investigate transepithelial ionic permeation via the paracellular pathway of human Caco-2 epithelial monolayers and its contribution to absorption of the base guanidine.

Methods. Confluent monolayers of Caco-2 epithelial cells were mounted in Ussing chambers and the transepithelial conductance and electrical potential difference (p.d.) determined after NaCl dilution or medium Na substitution (bi-ionic conditions). Guanidine absorption (J_{a-b}) was measured ± transepithelial potential gradients using bi-ionic p.d.'s.

Results. Basal NaCl replacement with mannitol gives a transepithelial dilution p.d. of 28.0 ± 3.1 mV basal solution electropositive (P_{Cl}/P_{Na} = 0.34). Bi-ionic p.d.'s (basal replacements) indicate a cation selectivity of $NH_4^+ > K^+ \sim Cs^+ > Na^+ > Li^+ >$ tetraethylammonium$^+ >$ *N*-methyl-D-glucamine$^+ \sim$choline$^+$. Transepithelial conductances show good correspondence with bi-ionic potential data. Guanidine J_{a-b} was markedly sensitive to imposed transepithelial potential difference. The ratio of guanidine to mannitol permeability (measured simultaneously) increased from 3.6 in the absence of an imposed p.d. to 13.8 (basolateral negative p.d.).

Conclusions. Hydrated monovalent ions preferentially permeate the paracellular pathway (Eisenman sequence 2 or 3). Guanidine may access the paracellular pathway because absorptive flux is sensitive to the transepithelial potential difference. An alternative method to assess paracellular-mediated flux of charged organic molecules is suggested.

KEY WORDS: Caco-2; cation selectivity; human intestine; organic cation absorption; paracellular pathway.

INTRODUCTION

Solute permeation across epithelial barriers is dependent upon both the permselective properties of the transcellular route and the noncellular (paracellular route) between epithelial cells (1–3). This is true of both monovalent cations and drugs in ''leaky'' epithelia (3–7).

The properties of the transcellular route have attracted most attention, the physiochemical properties of the phospholipid plasma membranes of apical and basal–lateral membranes providing a ready route for diffusion of hydrophobic compounds (3,7). However, the existence of plasma membrane carriers, exchangers (7–11), and channels (12) provides selective portals for hydrophilic molecules [e.g. peptide mimetics such as beta-lactam antibiotics, cephalosporins (9–11)], so enhancing absorption (9–11). Alternatively, active ATP-dependent pumps such as MDR-1 may render epithelial barriers effectively impermeable to their (hydrophobic) substrates (7,13).

The paracellular route consists of the rate-limiting tight junctional complex and a tortuous lateral space (3). The tight junction is considered to be a size-restricted route for permeation of hydrophilic molecules but which may allow passage of ions especially in low-resistance "leaky" epithelia (1,3,7,14,15). The ionic permselectivity of tight junctions may be critical to function in certain epithelia, such as the small intestine where selective cation permeability ensures that the majority of epithelial conductance and transepithelial Na^+ movement is not transcellular but rather passes between the cells via the paracellular pathway (4–6). Recently, mutations in proteins that localize to tight junctions (e.g. paracellin) and which give rise to human disease (familial hypomagnesemia) have demonstrated that the bulk of renal divalent cation absorption is paracellular and driven by the potential difference established by active transcellular NaCl absorption (16). In addition, change in paracellular conductance has been documented in intestinal inflammation and in chronic disease states such as Crohn's disease (13,17–19).

[1] Institute for Cell and Molecular Biosciences, Medical School, University of Newcastle upon Tyne, Framlington Place, Newcastle upon Tyne, NE2 4HH, UK.
[2] To whom correspondence should be addressed. (e-mail: n.l.simmons@ncl.ac.uk)

ABBREVIATIONS: EVOM, epithelial volt-ohm meter; J_{a-b}, transepithelial flux from apical to basal bathing solution; P_x, ionic permeability (for ion x); Ψ, p.d., transepithelial p.d. (mV); R_t, transepithelial electrical resistance.

Various criteria have been used to discriminate between paracellular and cellular routes; these include similar behavior to extracellular marker molecules (mannitol, polyethylene glycols, dextrans, and Lucifer yellow), the symmetry of bidirectional permeability coefficients with no evidence of saturable transport, and the ability to increase permeation following monolayer perturbation by chelating agents (7,15,18,20).

Such criteria may not be adequate for determining the route of transepithelial permeation of endogenous bases (thiamine, choline, guanidine) and equivalent charged basic drug molecules in native epithelia because a standing transepithelial potential difference (p.d.) generated by active transport (e.g. Na^+) may influence permeation via the "paracellular" route in "leaky" cation-selective epithelia such as the small intestine (7,8). On the basis of the passive diffusion of weak organic acids and bases, Adson *et al.* (21) proposed that the paracellular route in human Caco-2 epithelial layers comprised a 12-Å pore with a negatively charged weak electrostatic field, although heterogeneity in pore population size [3.7- or 4.5-Å restrictive pore combined with a nonrestrictive route (20,22), respectively] has been reported. The assumption that the fixed negative charge of the paracellular route confers preferential permeability to the charged cationic weak base has also been used to explain the pH-dependent permeability of such weak bases (23).

Early work by Frizzell and Schultz (4) and Schultz and Zalusky (5) used bi-ionic and dilution potentials to define the permselectivity properties of low-transepithelial-resistance rabbit ileum. It is likely that the paracellular pathway of both human jejunum and ileum are cation selective on the basis of measurements of dilution potentials elicited *in vivo* by nonelectrolytes (24,25); but, an extended experimental analysis of human small intestine does not yet exist. Many studies have used the Caco-2 cell system as an *in vitro* model for human small intestinal permeation (e.g. 7,8–11,13). However, no equivalent data to that measured in rabbit ileum exist. A main aim of the present paper is therefore to define the permselectivity properties of the paracellular pathway of Caco-2 epithelia to determine its similarity, or otherwise, to human small intestine. Second, using the method of Frizzell and Schultz (4) to partition paracellular flux from cellular movements by imposing external voltages and measuring the voltage sensitivity of transepithelial ion movements, we demonstrate that the transepithelial flux of the endogenous permanent base guanidine is markedly voltage sensitive as compared to transepithelial mannitol flux. We propose that the voltage sensitivity of transepithelial flux of charged organic solutes may be an additional and convenient method to allow partitioning of transepithelial flux to the paracellular route.

METHODS

Cell Culture

Caco-2 cells were originally obtained from Dr. I. Hassan (Ciba-Geigy Pharmaceuticals, Horsham, Sussex, UK); secondary stocks stored in liquid nitrogen (denoted MB90, i.e. 90 passage) were used between passage numbers 92 to 114. Cells were cultured in Dulbecco's modification of minimal essential medium containing glucose (4.5 g l^{-1}) and supplemented with nonessential amino acids (1%), L-glutamine (2 mM), fetal calf serum (10%), and gentamycin (30 μg ml^{-1}). Cell monolayers were prepared by seeding at high density (5.0×10^5 cells cm^{-2}) onto tissue culture inserts (Transwell 3401, 12-mm-diameter, 0.4 μm pore size uncoated polycarbonate filters, Costar, or Snapwell 3802, 12 mm-diameter, 3 μm pore size uncoated polycarbonate filters, Costar, Corning Inc, Corning, NY, USA). Cell monolayers were maintained at 37°C in a hum-idified atmosphere of 5% CO_2 in air. The culture medium was changed every 3 to 4 days. Experiments were performed 14 to 28 days after seeding and 18 to 24 h after feeding. Similar transepithelial resistance values (R_t) between the 3 μm pore size Snapwell and 0.4 μm pore size Transwell filters were observed [234 ± 16 Ω cm^2 (n = 18) *vs.* 172 ± 8 Ω cm^2 (n = 24), respectively] indicating that cell substrate and tortuous path considerations had a minimal effect in determining transepithelial resistance measurements (26).

Measurements of Transepithelial Electrical Potential Difference and Resistance

Cultured Snapwell epithelial layers were mounted in Ussing-type chambers maintained at 37°C, connected to an automatic voltage clamp (DVC-1000, World Precision Instruments, New Haven CT, USA) via saturated KCl/agar salt bridges (1.5 mm i.d.) and reversible electrodes (Ag/AgCl for current passage, calomel for voltage sensing). Measurements of open-circuit electrical potential difference were made at zero current, and transepithelial resistance (R_t) was measured by brief (2 s) DC current excursions of 50 μA in a hyperpolarizing direction (basal solution electropositive) in a 20 s cycle time. The use of saturated (3 M) KCl–agar bridges minimizes junction potentials that arise when asymmetric solutions are used (25). Filter resistance of 76 ± 9 Ω cm^2 (n = 6), measured identically, is subtracted from this data. Alternatively, in flux experiments transepithelial voltage and resistance were determined at 37°C using a volt-ohm meter fitted with "chopstick" electrodes (WPI EVOM, World Precision Instruments, New Haven CT, USA), which uses Ag/AgCl electrodes in contact with the solutions and square wave current pulses ± 20 μA at 12.5 Hz. Filter resistance of 92 ± 8 Ω cm^2 (n = 6), measured identically, is subtracted from this data. For Ag/AgCl electrodes, large junction potentials would be present arising from asymmetric Cl^- concentrations if dilution potentials were elicited using mannitol substitutions (27). Accordingly, where a transepithelial potential difference was established (see the next section) to drive transepithelial guanidine fluxes, bi-ionic Na:*N*-methyl-D-glucamine conditions were used (27). Comparison of the bi-ionic p.d's measured using the Ussing chamber (3 M KCl agar bridges) with the $Ag/AgCl_2$ epithelial volt-ohm meter (EVOM) electrodes (Table I *vs.* Fig. 3) gave similar basolateral positive values of 16–25 mV, respectively. The relative permeability ratio P_x/P_{Na} was calculated from the following equation (12):

$$P_x/P_{Na} = [Na]_a/[X]_a \cdot \exp(\Delta\Psi \cdot F/RT)$$

Table I. Dilution and Bionic Potentials Elicited by Basolateral NaCl Replacement

Basolateral solution	$\Delta\Psi$ (mV)	P_x/P_{Na}	G_T (mS cm^2)
NaCl	0	1.00	5.12 ± 0.3
Mannitol	28.0 ± 3.1	0.34[a]	–
NMDG Cl	15.9 ± 2.0	0.54	1.65 ± 0.21
Choline Cl	13.9 ± 1.8	0.58	1.61 ± 0.19
TEA Cl	13.2 ± 1.6	0.51	2.19 ± 0.17
LiCl	3.5 ± 0.3	0.87	4.54 ± 0.25
CsCl	−2.1 ± 0.2	1.08	4.92 ± 0.32
KCl	−3.1 ± 0.3	1.12	5.08 ± 0.45
NH_4Cl	−7.8 ± 0.5	1.34	5.74 ± 0.30

Dilution and bionic potentials elicited by replacement of the basolateral NaCl (137 mM) with various monovalent salts or isosmotic mannitol (274 mM) for epithelial layers mounted in Ussing chambers. The change in p.d. ($\Delta\Psi$) is expressed in millivolts. Epithelial conductance ($G_t = 1/R_t$) was determined from 50 μA current pulses in respective substituted modified Krebs solution. Ion selectivities were calculated as described in "Methods." Data are the mean ± SEM of ten Caco-2 cell monolayers.
NMDG, *N*-methyl-D-glucamine; TEA, tetraethylammonium.
[a] P_{Cl}/P_{Na}.

where X is the monovalent cation substitute and *a* refers to the apical concentrations of the cation. For dilution potentials, [Na] and [X] are the basal Na^+ and Cl^- concentrations, respectively. $\Delta\Psi$ is the change in p.d. from the NaCl-modified Krebs solution, *F* is the Faraday constant, *R* the gas constant, and *T* the temperature in Kelvin (12).

Transepithelial Transport Experiments

Transepithelial transport experiments were performed 14–21 days after seeding in Transwell filter supports and 18–24 h after feeding. Transepithelial flux measurements were performed essentially as described previously (9–11). Briefly, the cell monolayers were washed by immersion in four sequential beakers containing 200 mL modified Krebs buffer (see "Solutions"), placed in six-well plates, and 0.5 or 1 mL of modified Krebs buffer was added to apical and basal chambers, respectively, for 10 min at 37°C. Note that the Na^+ composition of the apical and basal chambers were modified by replacement of NaCl by equimolar substitutions with *N*-methyl-D-glucamine Cl (see "Solutions") to provide an electrical driving force across the epithelium. Otherwise, the compositions of the buffers in the apical and basal chambers were identical. Radiolabeled [^{3}H]mannitol (New England Nuclear) and [^{14}C]guanidine (0.1 μCi ml^{-1}, Amersham Biosciences) were added to the apical chamber with equal concentrations of 10 mM unlabeled substrates present in both apical and basal chambers. After a 20 min equilibration period, fluxes were measured in consecutive periods of up to 1 h so that the effects of transepithelial voltage imposition could be assessed in a paired manner on individual cell monolayers by replacement of the basal bathing solution. Samples were taken from apical or basal solutions (50 μL) at the end of each flux period. Fluxes are expressed as micromoles per centimeter squared per hour. Mannitol flux determinations are used to assess the magnitude of the passive (paracellular) component (9–11).

Microscopy

Caco-2 cell monolayers were washed in modified Krebs buffer and then fixed in 2% paraformaldehyde in modified Krebs buffer overnight at 4°C. After washing in Krebs solution, cells were permeabilized in 0.1% Triton X-100/Krebs for 15 min, washed again and stained with 2 μg cm^{-3} FITC–phalloidin for 60 min at room temperature, washed and mounted in Krebs solution, and visualized using a Leica laser scanning confocal microscope.

Solutions

A modified Krebs buffer solution was used for transepithelial electrical measurements of epithelial layers and measurement of transepithelial fluxes: (all mmol L^{-1}) NaCl 137, KCl 5.4, $CaCl_2$ 2.8, $MgSO_4$ 1.0, NaH_2PO_4 0.3, KH_2PO_4 0.3, glucose 10, HEPES/Tris 10 (pH 7.4, 37°C). For measurements of bi-ionic potentials elicited across the cation-selective paracellular pathway, equimolar substitutions of NaCl were made by *N*-methyl-D-glucamine Cl, choline Cl, LiCl, tetraethylammonium Cl, CsCl, KCl, and ammonium Cl. Isosmotic replacement of NaCl by mannitol (274 mM) was also used to measure the NaCl dilution potential.

Statistics

Data are expressed as mean values ± SEM for *n* separate epithelial layers. Significance of difference between mean values was determined using ANOVA with Bonferroni corrections for multiple comparisons applied to Student's *t* test (unpaired data) or for tests between individual data pairs (where appropriate). The level of significance was set at $p \leq 0.05$.

RESULTS

Transepithelial measurements of epithelial resistance (R_t) for Caco-2 cell monolayers grown under standard conditions to give confluent cell monolayers, whose phenotype includes Na-linked and proton-linked solute cotransporters typical of human small intestine (9–11), gave values between 200 and 300 Ω cm^2. In the present study for 18 cell layers mounted in Ussing chambers, the mean R_t was 234 ± 16 Ω cm^2, while the spontaneous p.d. (Ψ) was 0.66 ± 0.08 mV (basolateral solution electropositive). These data are consistent with early measurements showing a lack of electrogenic ion transport in basal conditions (28) and with an equivalent circuit analysis that is consistent with the majority of transepithelial conductance being associated with a noncellular paracellular conductance pathway (28).

Establishment of a NaCl gradient across the Caco-2 epithelium is associated with the generation of an electrical potential difference; when the basolateral NaCl is replaced with an isosmolar mannitol solution, the basolateral solution becomes markedly electropositive with respect to the apical solution (Table I), consistent with the existence of a cation-selective pathway. Calculation of the relative permeability for P_{Cl}/P_{Na} gives a value of 0.34. Upon the establishment of

bi-ionic conditions with sequential dilution of the basolateral solution NaCl with choline Cl, a potential difference of identical polarity to mannitol is observed (Fig. 1 and Table I), confirming that the pathway is selective for Na^+ over choline$^+$. This selectivity ratio is poor compared to transmembrane K^+ and Na^+ channels (12,29). A series of cations has been tested and the magnitude and polarity of the bi-ionic p.d. measured (Table I); whereas choline$^+$ and *N*-methyl-D-glucamine$^+$ elicit basolateral positive p.d.'s, Cs^+, K^+, and NH_4^+ elicit p.d.'s of the opposite polarity. Calculation of the relative P_{cation}/P_{Na} ratios are shown in Table I, which gives a cation selectivity sequence of $NH_4^+ > K^+ \sim Cs^+ > Na^+ > Li^+ >$ tetraethylammonium$^+ >$ *N*-methyl-D-glucamine$^+ \sim$choline$^+$. This sequence is an Eisenman sequence 2 or 3, indicating that the pathway is determined by a selectivity filter of low electrostatic field strength where ions permeate according to their hydrated radii, rather than the atomic radii (29). An interesting feature of the bi-ionic potential difference calculations is the finite permeability to *N*-methyl-D-glucamine$^+$ (molecular weight of Cl salt 195) and choline$^+$ (molecular weight 139) relative to Na^+, supporting the idea that the paracellular pathway may be accessed by a range of nutrient and pharmaceutically relevant molecules of similar molecular dimensions.

Table I shows conductance values for Caco-2 epithelial monolayers determined using current passage when bathed in modified Krebs solution where the NaCl has been substituted. On replacement of NaCl with mannitol or *N*-methyl-D-glucamine Cl, it can be seen that the majority of transepithelial conductance is dependent upon Na^+. Since there is no electrogenic transcellular transport of Na^+ (due to the low spontaneous p.d.; see the previous paragraphs), this is confirmatory evidence that the paracellular conductance is the main determinant of transepithelial conductance. There is good correspondence between the data from bi-ionic potentials and that from conductance demonstrating that ion conductance and selectivity are derived from the same pathway (29). If transcellular conductance pathways (for Na^+ and K^+ for instance) were the predominant transepithelial permeation pathways, highly selective ion channels (of higher field strength) would give quite different patterns of selectivity and conductance (29).

Figure 1 shows an unexpected feature in the Na^+:choline$^+$ bi-ionic potentials in that the p.d. elicited when apical NaCl is replaced, although of opposite sign, is smaller than that seen for equivalent basal solution replacements. This behavior is also observed for *N*-methyl-D-glucamine$^+$ replacements, basolateral replacement of 137 mM NaCl giving rise to a p.d. of 23.3 ± 1.7 mV, whereas apical replacement gave only −13.3 ± 0.9 mV (n = 12 monolayers) ($p < 0.01$, paired data). Therefore, it seems that the paracellular pathway of human Caco-2 epithelia does not behave in a strictly linear fashion with respect to Na^+-gradient-dependent p.d's.

As transepithelial resistance is markedly dependent upon cell shape and density (1), FITC–phalloidin staining of confluent monolayers of Caco-2 cells was performed to estimate linear junction density. Imaging of the cells at the subapical perijunctional actin ring (not shown) allows the determination of the linear junction density; this is 18.4 m cm^{-2} of epithelial surface area.

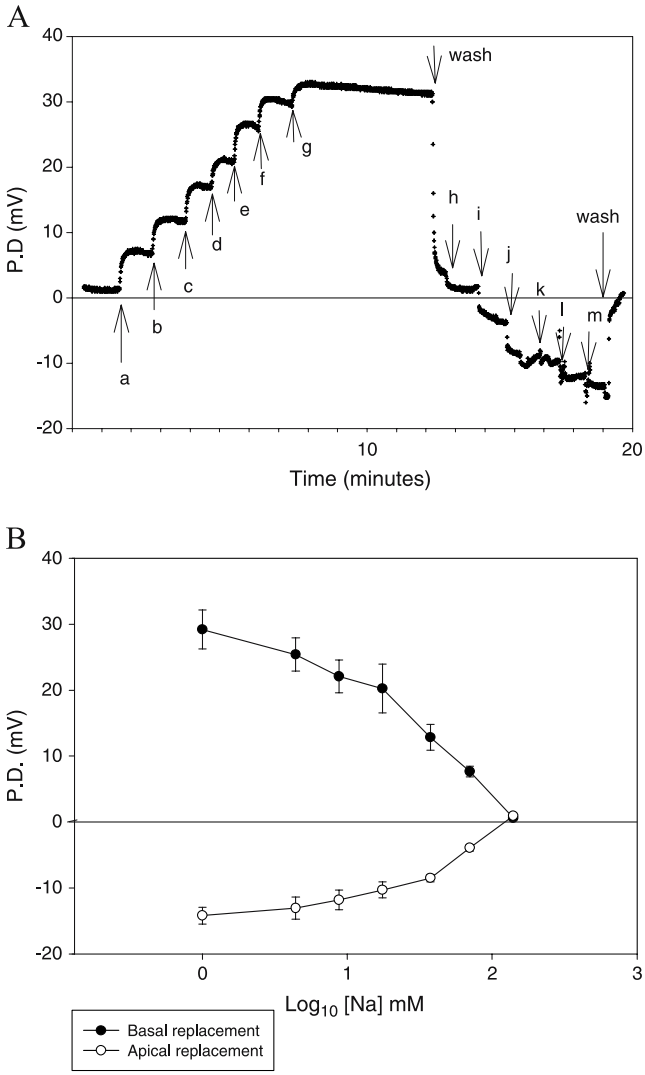

Fig. 1. (A) Continuous recording of transepithelial potential difference Ψ (P.D.) across a Caco-2 cell monolayer mounted in an Ussing chamber during which time the NaCl of the basolateral bathing solution was sequentially replaced by increasing concentrations of choline Cl (a–g). Note the slow decline in the bi-ionic Ψ at g. After washing and replacement of the basal bathing solution by normal NaCl, the P.D. rapidly returned toward the starting P.D. Replacement of the apical bathing solution NaCl with choline Cl (h–m) results in the development of a Ψ with an opposite sign. Ψ is expressed relative to the apical bathing solution (= 0). (B) Mean data for Na:choline bi-ionic potential differences recorded as in (A). Data are the mean ± the SEM of four to six Caco-2 cell monolayers.

Transcellular fluxes of the organic base guanidine (8) in Caco-2 cells have been observed to be mediated by transporters of relatively high affinity. Bidirectional fluxes of [^{14}C]guanidine were therefore determined at 0.1 and 10 mM to assess the magnitude of an active component. J_{a-b} was similar to J_{b-a} at both concentrations with no evidence for an active secretion or absorption [19.4 ± 1.2 and 18.1 ± 0.5 nmol cm^{-2} h^{-1} for 0.1 mM (both n = 3, not significant), and 2.00 ± 0.07 and 1.96 ± 0.12 μmol cm^{-2} h^{-1} for 10 mM (n = 3, not significant), respectively]. Transepithelial guanidine permeability was also not dependent upon guanidine concentration (P_{a-b}, 0.19 *vs.* 0.20 cm h^{-1} at 0.1 and 10 mM,

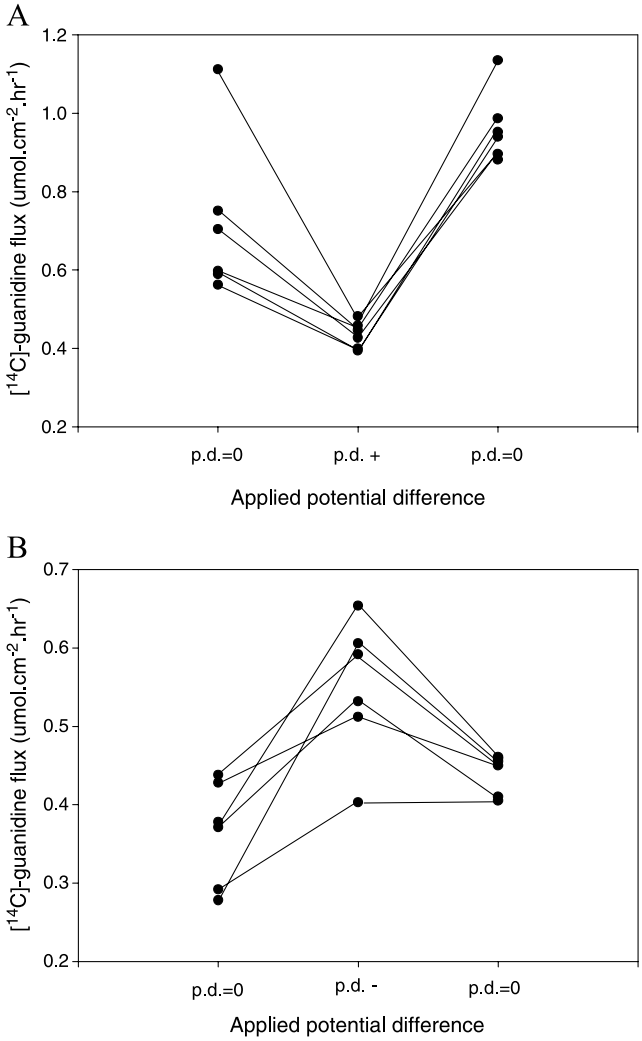

Fig. 2. Effect of an imposed transepithelial p.d. (Ψ_{a-b}) upon [^{14}C]guanidine fluxes from apical to basal solutions. Individual Caco-2 epithelial layers are connected by solid lines. (A) Fluxes were determined with an apical Na^+-containing modified Krebs solution. In the control 1-h period following a 20-min equilibration, an equivalent solution was present in the basal bathing solution. In the second 1 h period, a low-Na^+, *N*-methyl-D-glucamine$^+$–modified Krebs solution was present in the basolateral bathing solution, which generated an initial basolateral positive Ψ of 25.2 ± 2.8 mV, measured using EVOM (see "Methods"). A final control 1 h period completed the sequence. (B) Fluxes were determined with the *N*-methyl-D-glucamine$^+$ modified Krebs solution. A first control period with an equivalent basolateral solution was followed by a second period in which a Na-rich Krebs solution was present in the basolateral solution, which generated an initial basolateral negative Ψ of −17.6 ± 1.4 mV.

respectively). The inclusion of 0.1 mM verapamil did not substantially alter bidirectional transepithelial fluxes (not shown). In these conditions, we conclude that transcellular pathways contribute little to transepithelial guanidine fluxes. At 10 mM, guanidine transport systems of moderate or high affinity will be saturated (8) and their contribution to transepithelial flux minimal.

The ability to generate an electrical p.d. across an intact epithelium by dilution or bi-ionic p.d.'s allows the effect of the electrical gradient upon paracellular fluxes to be examined. Flux of the charged permanent organic base guanidine has been compared to the neutral sugar mannitol (9–11). In Na^+-containing media in the absence of an imposed p.d., J_{a-b} was 0.71 ± 0.08 (n = 6) μmol cm^{-2} h^{-1}, which exceeded J_{a-b} measured in solutions containing *N*-methyl-D-glucamine$^+$ of 0.36 ± 0.03 (n = 6) μmol cm^{-2} h^{-1} ($p < 0.01$). The Na^+-dependent flux may represent either transcellular transport or represent an effect of ionic composition on paracellular flux (see "Discussion"). More importantly, Fig. 2A and B illustrate that there is a marked effect of imposing either a positive or negative electrical p.d. (with respect to the apical bathing solution) upon guanidine fluxes, a positive potential decreasing guanidine flux [to 0.43 ± 0.01 μmol cm^{-2} h^{-1} (n = 6), $p < 0.01$ *vs.* first control period], whereas a negative transepithelial potential increasing guanidine flux [to 0.55 ± 0.04 (n = 6) μmol.cm^{-2} h^{-1}, $p < 0.01$ *vs.* control period in *N*-methyl-D-glucamine$^+$ media]. These effects were largely reversible on return to control conditions (Fig. 2A, B).

To separate active (transcellular) and passive (paracellular) Na^+ transport across rabbit ileum, Schultz and Zalusky (5) showed that voltage-driven Na^+ flux mediated through the paracellular pathway was a linear function of potential [$\exp(F/RT\Psi_{a-b})^{1/2}$] with an intercept representing the non-voltage-sensitive, cellular pathway. To estimate a linear function, data replicates at just two different potentials are sufficient to describe the mathematical relationship. Figure 3 shows such a plot for the data in Fig. 2 showing that there are differing slopes for the Na^+ data and for *N*-methyl-D-glucamine$^+$ data [0.83 ± 0.24 (SE) and 0.39 ± 0.13 (SE), respectively]. A positive intercept in this plot would indicate the magnitude of the potential-insensitive (transcellular) flux; in both data sets the intercept is not significantly different from zero [−0.11 ± 0.21 (SE), not significant, $p > 0.5$; −0.01 ± 0.16 (SE), not significant, $p > 0.9$,

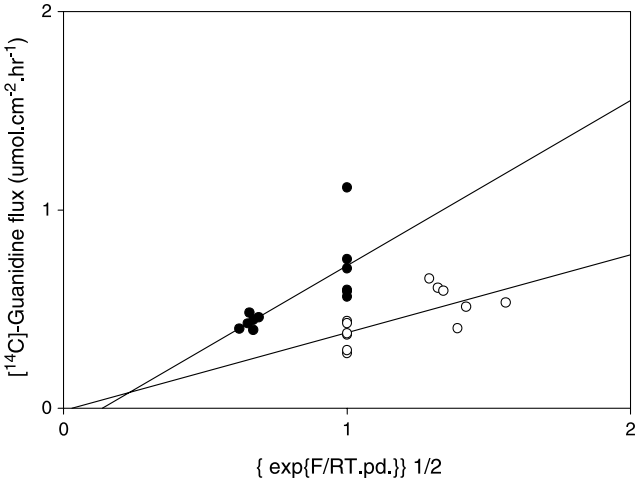

Fig. 3. Voltage dependence of [^{14}C]guanidine fluxes from apical to basal solutions. Individual values of [^{14}C]guanidine fluxes are plotted against the function $[\exp(F/RT\Psi_{a-b})]^{1/2}$. Closed circles were determined with Na^+-rich media present in the apical medium. Open circles are for *N*-methyl-D-glucamine$^+$–modified Krebs solution present in the apical media. Solid lines are the linear regression lines for the data: Ja−b = 0.83 ± 0.24 $\{\exp\{F/RT.\ \Psi a-b\}\}^{1/2}$−0.11 ± 0.21, r^2 = 0.52, $p < 0.05$ (Na-data), Ja−b = 0.39 ± 0.13 $\{\exp\{F/RT.\ \Psi a-b\}\}^{1/2}$−0.01 ± 0.16, r^2 = 0.46, $p < 0.05$ (N-methyl-D-glucamine$^+$).

respectively], confirming that there is little contribution from transcellular components to transepithelial flux under the conditions used (see "Discussion").

Comparison of the intrinsic permeability of guanidine to that of mannitol measured simultaneously (Table II) shows that the positively charged guanidine is 3.6-fold greater than neutral mannitol in the absence of an imposed basolateral negative p.d. Imposition of the negative bi-ionic p.d. accelerates guanidine flux but is without effect upon the mannitol flux, the guanidine/mannitol flux ratio increasing to 13.8-fold.

Finally, an additional test of paracellular permeation has been the covariation of a test compound with that of the inert transepithelial marker, mannitol. Figure 4 demonstrates that this is the case for guanidine flux. Epithelial layers, which show increased paracellular permeability by an elevated mannitol flux, also show a proportionally increased effect of imposed transepithelial p.d.

Taken together, these data confirm that small hydrophilic molecules may be subject to transintestinal absorption by a size-restricted, cation-selective paracellular pathway. The existence of a transepithelial p.d. (however generated) will significantly accelerate or retard charged solute movement via the paracellular pathway (see "Discussion"). An *in vitro* test of the paracellular permeation of a pharmacologically relevant base across Caco-2 epithelial layers may therefore include the effect of imposed voltages on absorptive permeation.

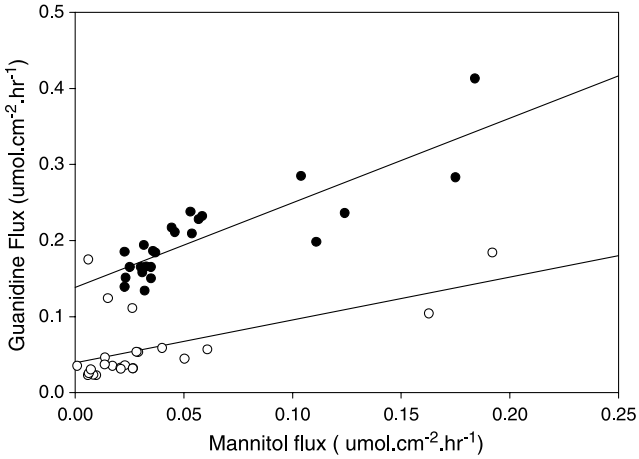

Fig. 4. Scatter plot showing the interrelationship between intrinsic paracellular permeability as monitored by transepithelial mannitol flux, transepithelial potential difference, and the transepithelial flux of guanidine. Open circles are for Ψ = 0 mV and solid circles are for Ψ held at negative values (with respect to the apical bathing solution). Other details as for Table II. Solid lines are linear regression lines for each data set.

DISCUSSION

Comprehensive data on the permselective properties of small intestinal mucosae is available for isolated rabbit ileum (4–6). In this low-resistance leaky epithelium, transepithelial Na^+ movement is determined mainly by the existence of a high-conductance paracellular pathway showing cation selectivity (4–6). Mucosal or serosal NaCl dilution elicits large transepithelial electrical potential differences due to this selectivity (6). Similar detailed measurements of human ileum are not available. Perfusion of the lumen of various segments of the human intestine using D-mannitol to generate diffusion potentials provides data on permselectivity (24,25). In the jejunum, the mucosae were highly permeable to NaCl movement, the pathway showing modest cation selectivity (24). In the ileum, this pathway was more cation selective (24). Opposite selectivity was observed in colon, with mucosae appearing to be overall anion selective (24). With these limited data, it seems that the human small intestine may display a paracellular pathway with similar characteristics to *in vitro* preparations of rabbit ileum.

Table II. Effect of an Imposed Transepithelial Potential Difference (Ψ) Upon [^{14}C]Guanidine Absorption

Substrate	Flux, J_{a-b} (μmol cm^{-2} h^{-1})	
	Ψ = 0 mV	Ψ = basolateral negative value
[^{14}C]Guanidine	0.204 ± 0.012	0.472 ± 0.025[a]
[^{3}H]Mannitol	0.056 ± 0.009	0.034 ± 0.010[b]

Effect of an imposed transepithelial p.d. (Ψ), basolateral solution electronegative upon [^{14}C]guanidine and [^{3}H]mannitol fluxes from apical to basal solutions. All fluxes were determined with low-Na^+, *N*-methyl-D-glucamine$^+$–modified Krebs solution in the apical solution. The basolateral solution was identical (Ψ = 0 mV) or contained the Na^+ Krebs solution (Ψ basolateral negative value, 20.7 ± 1.2 mV, n = 24, measured using EVOM; see "Methods"). All solutions contained 10 mM guanidine or mannitol. Fluxes at two transepithelial values of p.d were randomized; 12 epithelial layers had the negative p.d. imposed in the first flux period and held with equal solution composition thereafter or vice versa. Data are the mean ± SEM of 24 epithelial layers.

[a]Significantly different from zero Ψ.

[b]Not significant.

The transepithelial electrical properties of Caco-2 epithelia were originally described by Grasset *et al.* (28), who found values of transepithelial resistance (R_t) of ~150 Ω cm^2. In the present study, similar R_t values (~230 Ω cm^2) of fully differentiated Caco-2 cells were found, but these are higher than those for ileum (5,6). Such differences in resistance may result from the linear density of junctions per square centimeter of epithelium (1). In Caco-2 epithelia we have determined the linear junctional density to be 18.4 m cm^{-2}; this compares favorably to guinea pig/rat ileum villus enterocytes (31) and to other morphometric data for Caco-2 cells (14). It should be noted that the linear tight junction density of crypts exceeded that for villus enterocytes (77 *vs.* 22 m cm^{-2}), but the surface area of villus cells at 87% exceeded that for the crypts. However, it must be the case that for a flat monolayer culture, junctional density is smaller than seen in the folded villus structure of the native tissue (7). Alternative explanations relate to tight junctional strand number differences (31). However, because strand number is not correlated directly to morphological data (32), the exact contribution of villus and crypt to total conductance in the heterogeneous (human) ileum is not known.

The majority of transepithelial conductance will represent paracellular conductance in Caco-2 cell epithelia since equivalent circuit analysis of Caco-2 dome epithelia (28)

showed that the apical membrane resistance exceeded that for the basal membrane, which in turn were an order greater than the paracellular "shunt" resistance. Furthermore, Caco-2 cell input resistance is very high, ~1000 MΩ (33).

In studies of how enhanced transepithelial water flow might affect paracellular transport of small molecules in Caco-2 epithelia, Karlsson *et al.* (15) used hypotonic, glucose-rich apical (mucosal) solutions; these experimental conditions not only stimulated water flow but also generated a lumen positive diffusion potential in Caco-2 epithelial monolayers. This finding is equivalent to that seen *in vivo* for mannitol (24,25) and suggests that the Caco-2 paracellular pathway is cation selective. Using a variety of monovalent cation replacements in both the apical and basolateral bathing solutions, we demonstrate that the paracellular pathway is cation selective with a selectivity sequence of NH_4^+ > K^+~Cs^+ > Na^+ > Li^+ > tetraethylammonium$^+$ > *N*-methyl-D-glucamine~choline$^+$. This sequence order is an Eisenman sequence 2 or 3 (29), indicating that monovalent ions permeate in the hydrated state and that selectivity is determined by fixed anion sites of low field intensity. Therefore, Caco-2 epithelia display paracellular properties more similar to human ileum or fetal colon rather than adult colon (24). In studies of the dog kidney low-resistance, cation selective polarized Madin–Darby canine kidney (MDCK) II epithelial layers, a selectivity sequence of K^+ > Na^+ > Cs^+ > ~Li^+ was reported by Cereijido *et al.* (30) and more recently by Tang and Goodenough (34). This is an Eisenman sequence VI and VII of intermediate field strength (29). In both Caco-2 and MDCKII the ratio of selectivity between K^+ and Li^+ was low at 1.3. and 2.2, suggesting highly hydrated fixed anion sites within the paracellular pathway (30). Despite similar cation selectivity, differences must relate to the molecular architecture within the junctional complex. Recently, claudin 2 has been implicated in determining the cation selectivity of tight-junction channels in MDCK (35,36). Although claudin 2 is expressed in small intestine, it shows a crypt to villus decrease in expression (37). In Caco-2 epithelia, claudins 1, 3, and 5 were expressed, but claudin 2 was not (38). The exact basis for the molecular determination of cation-selective junctions for human intestinal Caco-2 epithelia remains to be determined.

Apical and basolateral transcellular transport mechanisms of guanidine have been described in Caco-2 cells (8). Guanidine was first presumed to be a P-glycoprotein substrate at low guanidine concentrations (8), and second uptake across both apical and basolateral membranes seems to occur via voltage-insensitive, high-affinity transporters of K_m values of 25 and 310 μM, respectively (8). Since transcellular transport is likely to be rate limited by the low-capacity apical transporter (8) any transcellular guanidine component will be small. The present data show that bidi-rectional transport rates are very similar and show no concentration dependence between 0.1 and 10 mM, confirming a minimal contribution of transcellular transport to guanidine transepithelial transport. Given the relative permeability difference between mannitol and guanidine (Table II), paracellular flux will be of significance at lower concentrations of guanidine than are used in the present study. Furthermore, the voltage sensitivity of the paracellular pathway contrasts to a lack of voltage sensitivity in Caco-2 cell membrane vesicles (8).

The present data utilizes bi-ionic potential differences elicited by Na^+:*N*-methyl-D-glucamine$^+$ to "voltage-clamp" Caco-2 cell layers without prolonged current injection. It is clear from the data that guanidine flux is voltage sensitive, being both accelerated and inhibited by transepithelial voltage. We propose that voltage sensitivity is an additional criterion to test permeation of charged solutes via the paracellular route. The intercept of a plot of $[\exp(F/RT\,\Psi_{a-b})]^{1/2}$ *vs.* flux shows that the transcellular component of guanidine is small relative to paracellular flux. Interestingly, flux from a Na^+-modified Krebs solution is higher than from a corresponding *N*-methyl-D-glucamine$^+$ modified Krebs solution, giving rise to an apparent Na^+ dependence at $\Psi = 0$. Since *N*-methyl-D-glucamine$^+$ shows a finite permeability relative to Na^+ (as assessed by bi-ionic p.d.'s) it is likely that *N*-methyl-D-glucamine$^+$ acts to block permeation of guanidine by competing with fixed anionic sites in the paracellular pathway. Such multi-ionic behavior is seen in tight-junction selective pores and is represented by behavior such as anomalous mole fraction conductance data (34). Since similar Px/P_{Na} values for choline and tetraethylammonium are observed (Table I) and because the nonhydrated molecular volume of these compounds is 113 and 158 Å^3 (39), we suggest that the paracellular pathway of Caco-2 cells has a size restriction of > 3.5 to < 5.4 Å radius. This is intermediate between the values in human gut and Caco-2 cells reported by Tavelin *et al.* (20) but very similar to that reported by Watson *et al.* (22). On the basis of such size restriction, paracellular permeation of weak basic hydrophilic drugs such as cimetidine (molecular radius 3.8 Å) (23,40) is clearly indicated. Ranitidine and famotidine not only permeate via the paracellular pathway in Caco-2 epithelia but also show a concentration-dependent block of epithelial (Na^+) conductance, consistent with binding to the fixed negative paracellular anionic sites and occlusion of the pore (41). Also in Caco-2 epithelia, negatively charged weak acids (chlorothiazide and furosemide, radii 3.6 and 3.9 Å, respectively) have lower intrinsic paracellular permeability than similar-sized cations of weak basic drugs (40).

The existence of a cation-selective, hydrophilic, size-restricted pathway for absorption of organic bases suggests that the pathway will be responsive to the transepithelial potential difference generated by transcellular transport. Since the absolute cation to anion selectivity is 0.34, weak organic acids and anions may also permeate the paracellular path in a voltage-dependent manner. In human ileum *in vivo* the spontaneous p.d. is ~12 mV lumen negative (25). Secretory and inflammatory stimuli will tend to increase the lumen negative potential difference by activation of CFTR. Nutrient absorption (e.g. sugars) will also increase the lumen negative potential difference by electrogenic Na^+-symport mechanisms. Further work needs to define the magnitude of change of lumen parameters on paracellular flux of cations likely to access the paracellular pathway *in vivo.*

CONCLUSION

The present study demonstrates that small hydrophilic molecules (e.g. permanent or weak bases) may be subject to transintestinal absorption by a size-restricted, cation-selective pathway. Under certain conditions, the paracellular pathway

may be the predominant pathway for absorption, but it will be markedly dependent upon the prevailing transepithelial p.d., which will accelerate or retard charged solute movement via the paracellular pathway. The potential sensitivity of absorptive flux of cationic drug molecules in Caco-2 (small intestinal) epithelia provides an additional test of paracellular permeation.

ACKNOWLEDGMENTS

Dr. C. Andersen supplied the Caco-2 epithelial layers (BBSRC grant 13/D17277). G. Carr performed the microscopy (Kidney Research UK). I. Haslam holds a BBSRC studentship.

REFERENCES

1. P. Claude. Morphological factors influencing transepithelial permeability: a model for the resistance of the zona occludens. *J. Membr. Biol.* **10**:219–232 (1978).
2. E. Fromter. The route of passive ion movement through the epithelium of Necturus gallbladder. *J. Membr. Biol.* **8**:259–301 (1972).
3. G. Kottra and E. Fromter. Functional properties of the paracellular pathway in some leaky epithelia. *J. Exp. Biol.* **106**:217–229 (1983).
4. R. A. Frizzell and S. G. Schultz. Ionic conductances of extracellular shunt pathway in rabbit ileum. Influence of shunt on transmural sodium transport and electrical potential differences. *J. Gen. Physiol.* **59**:318–346 (1972).
5. S. G. Schultz and R. Zalusky. Ion transport in isolated rabbit ileum; short circuit current and Na-fluxes. *J. Gen. Physiol.* **47**: 567–584 (1964).
6. N. L. Simmons and R. J. Naftalin. Bidirectional sodium ion movements via the paracellular and transcellular routes across short-circuited rabbit ileum. *Biochim. Biophys. Acta* **448**:426–450 (1976).
7. P. Artursson, K. Palim, and K. Luthman. Caco-2 monolayers in experimental and theoretical predictions of drug transport. *Adv. Drug Deliv. Rev.* **46**:27–43 (2001).
8. E. Cova, U. Laforenza, G. Gastaldi, Y. Sambuy, S. Tritto, A. Faelli, and U. Ventura. Guanidine transport across the apical and basolateral membranes of human intestinal Caco-2 cells is mediated by 2 different mechanisms. *J. Nutr.* **132**:1995–2003 (2002).
9. D. T. Thwaites, G. T. A. McEwan, C. D. A. Brown, B. H. Hirst, and N. L. Simmons. Na-independent, H-coupled transepithelial β-alanine absorption by human intestinal Caco-2 cell monolayers. *J. Biol. Chem.* **268**:18438–18441 (1993).
10. D. T. Thwaites, C. D. A. Brown, B. H. Hirst, and N. L. Simmons. Transepithelial Gly-Sar transport in intestinal Caco-2 cells mediated by expression of H^+-coupled carriers at both apical and basal membranes. *J. Biol. Chem.* **268**:7640–7642 (1993).
11. D. T. Thwaites, M. G. Cavet, B. H. Hirst, and N. L. Simmons. Angiotensin-converting enzyme (ACE) inhibitor transport in human intestinal epithelial (Caco-2) cells. *Br. J. Pharmacol.* **114**:981–986 (1995).
12. B. Hille. The permeability of the sodium channel to metal cations in myelinated nerve. *J. Gen. Physiol.* **59**:637–658 (1972).
13. J. Hunter, B. H. Hirst, and N. L. Simmons. Drug absorption limited by P-glycoprotein mediated secretory drug transport in human intestinal epithelial Caco-2 cell-layers. *Pharm. Res.* **10**:743–749 (1993).
14. A. Collett, D. Walker, E. Sims, Y. L. He, P. Speers, J. Ayrton, M. Rowland, and G. Warhurst. Influence of morphometric factors on quantification of paracellular permeability of intestinal epithelia *in vitro*. *Pharm. Res.* **14**:767–777 (1997).
15. J. Karlsson, A.-L. Ungell, J. Grasjo, and P. Artursson. Paracellular drug transport across intestinal epithelia: influence of charge and induced water flux. *Eur. J. Pharm. Sci.* **9**:47–56 (1999).
16. D. B. Simon, Y. Lu, K. A. Choate, H. Velazquez, E. Al-Sabban, M. Praga, G. Casari, A. Bettinelli, G. Colussi, J. Rodriguez-Soriano, D. McCredie, D. Milford, S. Sanjad, and R. P. Lifton. Paracellin-1, a renal tight junction protein required for paracellular Mg^{2+} resorption. *Science* **285**:103–106 (1999).
17. M. L. Marin, A. J. Greenstein, S. A. Geler, R. E. Gordon, and A. H. Aufses. A freeze fracture study of Crohn's disease of the terminal ileum: changes in epithelial tight junction organisation. *Am. J. Gastroenterol.* **78**:537–547 (1983).
18. J. D. Soderholm, G. Olaison, K. H. Peterson, L. E. Franzen, T. Lindmark, M. Wiren, C. Tageson, and R. Sjodahl. Augmented increase in tight junction permeability by luminal stimuli in the non-inflamed ileum of Crohn's disease. *Gut* **50**:307–313 (2002).
19. C. S. Hyun, C. W. Chen, N. L. Shinowara, T. Paaia, F. S. Fallick, L. A. Martello, M. Muennnudde, V. M. Donovan, and S. Teichberg. Morphological factors influencing transepithelial conductance in a rabbit model of ileitis. *Gastroenterology* **109**:13–23 (1995).
20. S. Tavelin, J. Taipalensuu, L. Soderberg, R. Morrison, S. Chong, and P. Artursson. Prediction of the oral absorption of low-permeability drugs using an intestine-like 2/4/A1 cell monolayers. *Pharm. Res.* **20**:397–405 (2003).
21. A. Adson, P. S. Burton, T. J. Raub, C. L. Barsuhn, K. L. Audus, and B. F. Ho. Passive diffusion of weak organic electrolytes across Caco-2 cell monolayers: uncoupling the contributions of hydrodynamic, transcellular and paracellular barriers. *J. Pharm. Sci.* **84**:1197–11204 (1995).
22. C. J. Watson, M. Rowl, and G. Warhurst. Functional modelling of tight junctions in intestinal cell monolayers using polyethylene glycol oligomers. *Am. J. Physiol.* **281**:C388–C397 (2001).
23. N. Nagahara, S. Tavelin, and P. Artursson. Contribution of the paracellular route to the pH-dependent epithelial permeability to cationic drugs. *J. Pharm. Sci.* **93**:2972–2984 (2004).
24. G. R. Davis, C. A. Santa Ana, S. G. Morawski, and J. S. Fordtran. Permeability characteristics of human jejunum, ileum, proximal colon: results of potential difference measurements and unidirectional fluxes. *Gastroenterology* **83**:844–850 (1982).
25. R. F. Gustke, P. McCormick, H. Ruppin, K. H. Soergel, G. E. Whalen, and C. M. Wood. Human intestinal potential difference: recording method and biophysical implications. *J. Physiol.* **321**:571–582 (1981).
26. C.-M. Lo, C. R. Keese, and I. Giaever. Cell–substrate contact: another factor may influence transepithelial electrical resistance of cell layers cultured on permeable supports. *Exp. Cell Res.* **250**:576–580 (1999).
27. P. H. Barry and J. P. Calc. A software package for calculating liquid junction potential corrections in patch-clamp, intracellular, epithelial and bilayer measurements and for correcting junction potential measurements. *J. Neurosci. Methods* **51**: 107–116 (1994).
28. E. Grasset, M. Pinto, E. Dussaulx, A. Zweibaum, and J.-F. Desjeux. Epithelial properties of human colonic carcinoma cell line Caco-2: electrical parameters. *Am. J. Physiol.* **247**: C260–C267 (1984).
29. G. Eisenman and R. Horn. Ion selectivity revisited: the role of kinetic and equilibrium processes in ion permeation through channels. *J. Membr. Biol.* **76**:197–225 (1983).
30. M. Cereijido, E. S. Robbins, W. J. Dolan, C. A. Rotunno, and D. D. Sabatini. Polarised monolayers formed by epithelial cells on a permeable and translucent support. *J. Cell Biol.* **77**:853–879 (1977).
31. M. A. Marcial, S. L. Carlson, and J. L. Madara. Partitioning of paracellular conductance along the crypt–villus axis: a hypothesis based on structural analysis with detailed consideration of tight-junction structure function relationships. *J. Membr. Biol.* **80**:59–70 (1984).
32. B. R. Stevenson, J. M. Anderson, D. A. Goodenough, and M. S. Mooseker. Tight junction structure and Zo-1 content are identical in two strains of Madin–Darby canine kidney cells which differ in transepithelial resistance. *J. Cell Biol.* **107**:2401–2408 (1988).
33. X.-Y. Tien, T. A. Brasitus, M. A. Kaetzel, J. R. Dedman, and D. J. Nelson. Activation of the cystic fibrosis transmembrane

conductance regulator by cGMP in the human colonic cancer cell-line, Caco-2. *J. Biol. Chem.* **269**:51–54 (1994).
34. V. W. Tang and D. A. Goodenough. Paracellular ion channel at the tight junction. *Biophys. J.* **84**:1660–1673 (2003).
35. S. Amasheh, N. Meiri, A. H. Gitter, T. Schoneberg, J. Mankertz, J. D. Schulz, and M. Fromm. Claudin-2 expression induces cation-selective channels in tight-junction of epithelial cells. *J. Cell Sci.* **15**:4969–4976 (2002).
36. C. M. Van-Itlaie, A. S. Fanning, and J. M. Anderson. Reversal of charge selectivity in cation or anion-selective epithelial lines by expression of different claudins. *Am. J. Physiol.* **285**: F1078–F1084 (2003).
37. C. Rahner, L. L. Mitic, and J. M. Anderson. Heterogeneity in expression and sub-cellular localization of claudins 2, 4 and 5 in the rat liver, pancreas and gut. *Gastroenterology* **120**:411–422 (2001).
38. J. McLaughlin, P. J. Padfield, J. P. Burt, and C. A. O'Neil. Ochratoxin A increases permeability through tight junctions by removal of specific claudin isoforms. *Am. J. Physiol.* **287**:C1412–C1417 (2004).
39. H. Ginsburg and W. D. Stein. The new permeability pathways induced by the malaria parasite in the membrane of the infected erythrocyte: comparison of results using different experimental techniques. *J. Membr. Biol.* **197**:113–122 (2004).
40. V. Pade and S. Stavchansky. Estimation of the relative contribution of the transcellular and paracellular pathway to the transport of passively absorbed drugs in the Caco-2 cell culture model. *Pharm. Res.* **14**:1210–1215 (1997).
41. K. Lee and D. R. Thakker. Saturable transport of H2-antagonists ranitidine and famotidine across Caco-2 cell monolayers. *J. Pharm. Sci.* **88**:680–687 (1999).